JOURNAL OF THERMOPHYSICS AND HEAT TRANSFER
Vol. 12, No. 3, July–September 1998

# Effects of Buoyancy on Electrohydrodynamic-Enhanced Forced Convection in a Horizontal Channel

F. C. Lai*
*University of Oklahoma, Norman, Oklahoma 73019*

**Buoyancy effects on heat transfer enhancement using an electrohydrodynamic (EHD) technique is numerically examined for laminar forced convection in a horizontal channel. Attention is also focused on the effect of added buoyancy on the flow stability. The flow Reynolds numbers and thermal buoyancy strength considered are in the range of $6 \times 10^2 \le Re \le 1.8 \times 10^3$ and $10^4 \le Gr \le 10^6$, respectively. The electrical field is generated by positive corona from a wire electrode charged with dc high-voltage ($10 \le V_0 \le 17.5$ kV). In terms of an EHD number, this corresponds to $0.36 \le N_{ehd} \le 23.56$. The results show that heat transfer enhancement increases with the applied voltage. For a given electric field, oscillation in the flow and temperature fields is observed for flows at small Reynolds numbers. In addition, the flow and temperature fields become more unstable with an increase in the thermal buoyancy strength. Because of the existence of secondary flows, there is an improvement in heat transfer. However, it is observed that thermal buoyancy has a negligible effect on the heat transfer enhancement for $Gr < 10^6$.**

## Nomenclature

$b$ = ion mobility of air, $m^2/V\ s$
$D_h$ = hydraulic diameter, m
$d$ = distance between wire and plate, m
$Gr$ = Grashof number, $g\beta(T_w - T_i)d^3/\nu^2$
$g$ = gravitational acceleration, $m/s^2$
$h$ = local heat transfer coefficient, $W/m^2\ s$
$\bar{h}$ = average heat transfer coefficient, $W/m^2\ s$
$k$ = thermal conductivity of air, $W/m^2\ s$
$\bar{L}$ = dimensionless channel length, $L/d$
$Nu$ = overall Nusselt number, $\bar{h}D_h/k$
$\overline{Nu}$ = time-averaged Nusselt number
$\overline{Nu_f}$ = time-averaged Nusselt number for forced convection with electric field
$Nu_x$ = local Nusselt number, $hD_h/k$
$Pe_{ehd}$ = Peclet number, $u_e d/\alpha$
$Re$ = flow Reynolds number, $2u_i d/\nu$
$Re_{ehd}$ = EHD Reynolds number, $u_e d/\nu$
$T_i$ = inlet air temperature, K
$T_w$ = wall temperature, K
$u_e$ = characteristic velocity of ionic wind, m/s
$u_i$ = uniform velocity at the inlet, m/s
$\bar{u}_i$ = dimensionless inlet velocity of air, $u_i/u_e$
$V$ = electric potential, V
$\bar{V}$ = normalized electrical potential, $V/V_0$
$V_0$ = electric potential at the wire, V
$\bar{x}, \bar{y}$ = dimensionless Cartesian coordinates, $x/d$ and $y/d$, respectively
$\alpha$ = thermal diffusivity, $m^2/s$
$\beta$ = coefficient of thermal expansion, 1/K
$\varepsilon$ = permittivity of air, F/m
$\theta$ = dimensionless temperature, $(T - T_i)/(T_w - T_i)$
$\theta_0$ = dimensionless mean outlet air temperature
$\nu$ = kinematic viscosity of air, $m^2/s$
$\rho$ = density of air, $kg/m^3$
$\rho_c$ = ionic space charge density, $C/m^3$
$\overline{\rho_c}$ = dimensionless space charge density, $\rho_c/\rho_{c0}$
$\rho_{c0}$ = ionic space charge density at the wire, $C/m^3$
$\tau$ = dimensionless time, $u_e t/d$
$\overline{\psi}$ = dimensionless stream function, $\psi/u_e d$
$\overline{\omega}$ = dimensionless vorticity, $\omega d/u_e$

Presented as Paper 97-0594 at the AIAA 35th Aerospace Sciences Meeting, Reno, NV, Jan. 6–9, 1997; received Oct. 7, 1997; revision received March 9, 1998; accepted for publication March 20, 1998. 

*Associate Professor, School of Aerospace and Mechanical Engineering. E-mail: lai@leo.enc.ou.edu. Senior Member AIAA.

## Introduction

ENHANCEMENT of heat transfer has been a subject of major interest for many decades. In terms of power consumption and maintenance requirements, the method involving electrohydrodynamics (EHD) seems to be the most attractive among available techniques. When air is the working fluid, the mechanism for EHD heat transfer enhancement arises from the electrically induced secondary flow, which is also known as ionic wind or corona wind. The EHD-induced secondary flow can be thought of as a gas stream issued from the charged electrode to the grounded heat transfer surface. The net effect of this secondary flow is additional mixing of the fluid and destabilization of the thermal boundary layer, thus leading to a substantial increase in heat transfer coefficient. Enhancement of heat transfer by EHD has been known for some time. Over the past three decades, an extensive amount of research has been devoted to the fundamentals of EHD-enhanced heat transfer, both experimentally and theoretically. Because excellent reviews of studies on this subject can be found in the literature,[1–3] they are omitted here for brevity.

Despite a general understanding of EHD operation and numerous successful applications in industry, many questions regarding the actual enhancement mechanism have remained unanswered. Because of the complications involved, previous studies were mainly based on experiments and primarily emphasized the role of the electric body force in the creation of secondary flows. Very limited numerical results have been reported on the interaction between the flow and electrostatic fields. The interaction of the electric wind with a superimposed external flow was first numerically investigated by Yamamoto and Velkoff.[4] The study was re-examined later by Lai et al.[5] to reveal the existence of steady periodic flows. Although the existence of EHD-induced oscillatory flows has also been observed by Takimoto et al.[6] in their experimental study of EHD flows, the relation among the oscillatory frequency, the Reynolds number, and the dimensionless EHD number was not fully disclosed until recently.[5] From the heat transfer point of view, it is speculated that the oscillatory flows thus generated may

lead to an increase in the heat transfer between the flowing air and the heat transfer surface. This speculation has been recently confirmed for forced convection in a horizontal channel charged by an electrode wire located at the center.[7] In addition, it has been reported that the resulting flow and temperature fields may become steady, steady periodic, and nonperiodic because of the interactions among the electric, flow, and temperature fields. To further investigate the mechanism for EHD-enhanced heat transfer, a recent study has been extended to include the effects of thermal buoyancy.[7] Thus, it is the objective of the present study to examine the effects of the added thermal buoyancy on the heat transfer enhancement and flow stability.

## Formulation and Numerical Method

The geometry considered is a two-dimensional horizontal channel. The channel walls that are maintained at a constant temperature $T_w$ are electrically grounded (Fig. 1). An electrode wire charged with dc high voltage is placed at the center of the channel. Only positive corona discharge is considered in the present study. Because the positive corona discharge is uniformly distributed along the length of the wire, it permits a two-dimensional analysis. Air at a uniform velocity $u_i$ and temperature $T_i (T_i > T_w)$ is introduced at the channel inlet. This channel, which has dimensions identical to that of the previous study,[4] is chosen so that the reported electric field data can be used as an input for the present numerical calculations.

For the problem considered, the governing equations of the electrical field are given by[5,7]

$$\frac{\partial^2 V}{\partial x^2} + \frac{\partial^2 V}{\partial y^2} = -\frac{\rho_c}{\varepsilon} \tag{1}$$

$$\rho_c^2 = \varepsilon \left( \frac{\partial \rho_c}{\partial x}\frac{\partial V}{\partial x} + \frac{\partial \rho_c}{\partial y}\frac{\partial V}{\partial y} \right) \tag{2}$$

with the boundary conditions given by

$$V = V_0, \quad \text{at the wire} \tag{3a}$$

$$V = 0, \quad \text{along the channel wall} \quad (y = \pm d) \tag{3b}$$

$$\frac{\partial V}{\partial y} = 0, \quad \text{along the horizontal centerline} \quad (y = 0) \tag{3c}$$

$$\frac{\partial V}{\partial x} = 0, \quad \text{along the vertical centerline} \quad (x = L/2) \tag{3d}$$

For parameters considered in the present study, the ion drift velocity is much higher than the air velocity such that the contribution of convective flow to the current density is neglected. Also, the electrodynamic and fluid dynamic equations can be decoupled for the same reason. Thus, the simplified forms of the Maxwell's equations and Ohm's law can be solved independently of the flowfield equations.

For the flow and temperature fields, the dimensionless governing equations in terms of the stream function and vorticity are given by[7]

$$\frac{\partial^2 \bar{\psi}}{\partial \bar{x}^2} + \frac{\partial^2 \bar{\psi}}{\partial \bar{y}^2} = -\bar{\omega} \tag{4}$$

$$\frac{\partial \bar{\omega}}{\partial \tau} = \frac{\partial \bar{\psi}}{\partial \bar{x}}\frac{\partial \bar{\omega}}{\partial \bar{y}} - \frac{\partial \bar{\psi}}{\partial \bar{y}}\frac{\partial \bar{\omega}}{\partial \bar{x}} + \frac{1}{Re_{ehd}}\left( \frac{\partial^2 \bar{\omega}}{\partial \bar{x}^2} + \frac{\partial^2 \bar{\omega}}{\partial \bar{y}^2} \right) + \left( \frac{\partial \bar{V}}{\partial \bar{y}}\frac{\partial \bar{\rho_c}}{\partial \bar{x}} - \frac{\partial \bar{V}}{\partial \bar{x}}\frac{\partial \bar{\rho_c}}{\partial \bar{y}} \right) + \frac{Gr}{Re_{ehd}^2}\frac{\partial \theta}{\partial \bar{y}} \tag{5}$$

$$\frac{\partial \theta}{\partial \tau} = \frac{\partial \bar{\psi}}{\partial \bar{x}}\frac{\partial \theta}{\partial \bar{y}} - \frac{\partial \bar{\psi}}{\partial \bar{y}}\frac{\partial \theta}{\partial \bar{x}} + \frac{1}{Pe_{ehd}}\left( \frac{\partial^2 \theta}{\partial \bar{x}^2} + \frac{\partial^2 \theta}{\partial \bar{y}^2} \right) \tag{6}$$

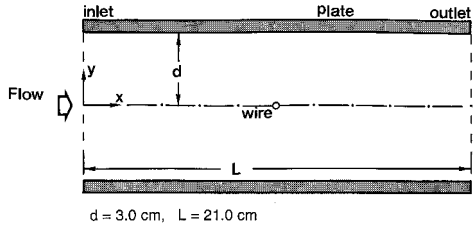


**Fig. 1 Horizontal channel with one electrode wire located at the center.**

where $Re_{ehd}$ and $Pe_{ehd}$ are both based on the electric characteristic velocity $u_e$ $(=\sqrt{\rho_{c0} V_0/\rho})$. While the fourth term on the right-hand side of Eq. (5) represents the body force term because of the electrical field, the last term represents the thermal buoyancy effect. For the geometry considered, the electric current involved is very small (on the order of $10^{-5}$ A, based on the measurements of Yamamoto and Velkoff[4]) over the range of voltage applied, which justifies the neglect of Joule heating.

The boundary conditions for the flow and temperature fields are given by

$$\bar{x} = 0, \quad \bar{\omega} = 0, \quad \bar{\psi} = \bar{u}_i \bar{y}, \quad \theta = 0 \tag{7a}$$

$$\bar{x} = \bar{L}, \quad \frac{\partial \bar{\omega}}{\partial \bar{x}} = 0, \quad \frac{\partial \bar{\psi}}{\partial \bar{x}} = 0, \quad \frac{\partial \theta}{\partial \bar{x}} = 0 \tag{7b}$$

$$\bar{y} = 1, \quad \bar{\omega} = \frac{\partial^2 \bar{\psi}}{\partial \bar{y}^2}, \quad \bar{\psi} = \bar{u}_i, \quad \theta = 1 \tag{7c}$$

$$\bar{y} = -1, \quad \bar{\omega} = \frac{\partial^2 \bar{\psi}}{\partial \bar{y}^2}, \quad \bar{\psi} = -\bar{u}_i, \quad \theta = 1 \tag{7d}$$

At the channel exit, gradients of stream function, vorticity, and temperature are set to zero. These boundary conditions are less restrictive and are widely accepted. To ensure that the physical phenomena observed are not affected by the channel length and boundary conditions applied at the exit, calculations have been performed on an extended domain ($L/d = 10$). As reported,[8] the flow and temperature fields thus obtained are nearly identical, and so is the period of oscillatory flows.

To evaluate the heat transfer performance, one needs to calculate the heat transfer coefficient. The local heat transfer coefficient in terms of the local Nusselt number is given by

$$Nu_x = \frac{hD_h}{k} = \frac{qD_h}{k(T_w - T_m)} = \frac{D_h \left( \dfrac{\partial T}{\partial y} \right)}{T_w - T_m} \tag{8}$$

In the preceding expression $D_h$ is the hydraulic diameter that is $4d$ for the present case, and $T_m$ is the fluid bulk temperature at the given location. The average heat transfer coefficient can thus be determined from the overall Nusselt number, which is given by

$$Nu = \frac{4}{\bar{L}} \frac{\log(1/\theta_0)}{1 - \theta_0} \int_0^{\bar{L}} \left. \frac{\partial \theta}{\partial \bar{y}} \right|_{\bar{y}=\pm 1} d\bar{x} \tag{9}$$

For the solution of the electric field, the numerical procedure employed to solve Eqs. (1) and (2) is identical to that used by Yamamoto and Velkoff.[4] Electric potential and space charge density are determined by iterating on Eqs. (1) and (2) with an assumed value of space charge density at the wire ($\rho_{c0}$). The validity of the solution is checked by comparing the predicted total current with the measured current at the corresponding voltage. If the currents do not match, a new value of space charge density at the wire is assumed and the calculations are repeated. The solutions of the flow and temperature fields are obtained using the standard procedure for the stream function–

vorticity formulation, which is well documented in most numerical textbooks and omitted here for brevity.

Numerical solution starts with the calculations of the electric field, it is then followed by solving the flow and temperature fields simultaneously. Uniform grid (225 × 65) is chosen for the present study, which is the same as those used in the previous analyses performed by Yamamoto and Velkoff[4] and Lai et al.[5] for the same channel configuration. The test of grid dependence has been reported in previous studies.[4,5] Because the radius of the electrode wire ($10^{-4}$ m) is small compared with the grid spacing used (9.375 x $10^{-4}$ m), it is appropriate to treat the wire as a nodal point. The dimensionless time step chosen is $5 \times 10^{-4}$ to guarantee numerical stability and accuracy. The stability criterion for the numerical scheme used is given by Jaluria and Torrance[9]

$$\Delta t \leq 1 \Big/ \left\{ 2\nu \left[ \frac{1}{(\Delta x)^2} + \frac{1}{(\Delta y)^2} \right] + \frac{|u|}{\Delta x} + \frac{|v|}{\Delta y} \right\} \qquad (10)$$

To verify that the observed oscillations are not a result of numerical instability, the computation has been repeated with a reduced time step ($\Delta\tau = 1 \times 10^{-4}$). The results obtained are identically the same with those using the time step of $\Delta\tau = 5 \times 10^{-4}$. Calculations covered a wide range of parameters ($10 \leq V_0 \leq 17.5$ kV, $6 \times 10^2 \leq Re \leq 1.8 \times 10^3$, and $10^4 \leq Gr \leq 10^6$), with particular attention being placed on the stability of the flow and temperature fields because of the added thermal buoyancy. To closely monitor the development of the flow and temperature fields, the computation is continued until a steady state or steady periodic state is reached. Most of the computations were performed on the Cray supercomputer J90, which takes about 8 h of CPU time for 500 dimensionless time periods. Some calculations were taken on the SUN SPARC 10 workstation, which requires about 50 h of CPU time for the same time period as the Cray supercomputer.

## Results and Discussion

To examine the interaction between the flow and electric fields, it is convenient to use a parameter that represents the ratio of electrical body force to flow inertia. For the present study, the parameter used is the EHD number proposed by Davidson and Shaughnessy,[10] which is given by

$$N_{ehd} = \frac{Id}{\rho u_i^2 bA} \qquad (11)$$

where $I$ is the total current and $A$ is the plate area. A high EHD number thus implies that either the flow Reynolds number is small or the applied voltage is large. The preceding definition of an EHD number is different from that used by Yamamoto and Velkoff,[4] which is given by

$$N_{ehd} = \frac{Re_{ehd}}{Re} = \frac{u_e}{2u_i} \qquad (12)$$

Because $u_e$ cannot be measured directly, the definition based on Eq. (11) is preferred over Eq. (12).

As reported earlier,[5,7] the flow and temperature fields in the presence of an electrical field may not always reach a steady state. In general, it is observed that the flow and temperature fields at a given electrical condition are oscillatory when the flow Reynolds number is small, i.e., at a high EHD number. A steady state can only be reached when the flow Reynolds number is sufficiently increased, i.e., at a small EHD number. Based on previous results the flow and temperature fields reach a steady state only at $V_0 = 10$ kV.[7] For other applied voltages, the flow and temperature fields may become steady or steady periodic, depending on the flow Reynolds number.

For the present study, the transition of flow and temperature fields become very complicated in the presence of thermal buoyancy. As shown in Fig. 2, the flow and temperature fields are always stable when $N_{ehd} < 2$, and become oscillatory (either periodic or non-periodic) when $N_{ehd} > 10$. No definite conclusion can be drawn on the flow stability when $2 < N_{ehd} < 10$. For a given Grashof number, it is observed that the flow and temperature fields change from a steady convection at a small EHD number to periodic and nonperiodic oscillation when the

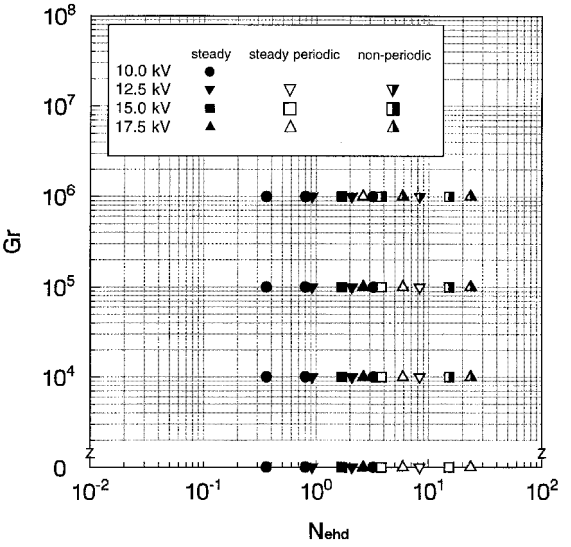


**Fig. 2 Transition of flow and temperature fields under the influence of electric field and thermal buoyancy.**

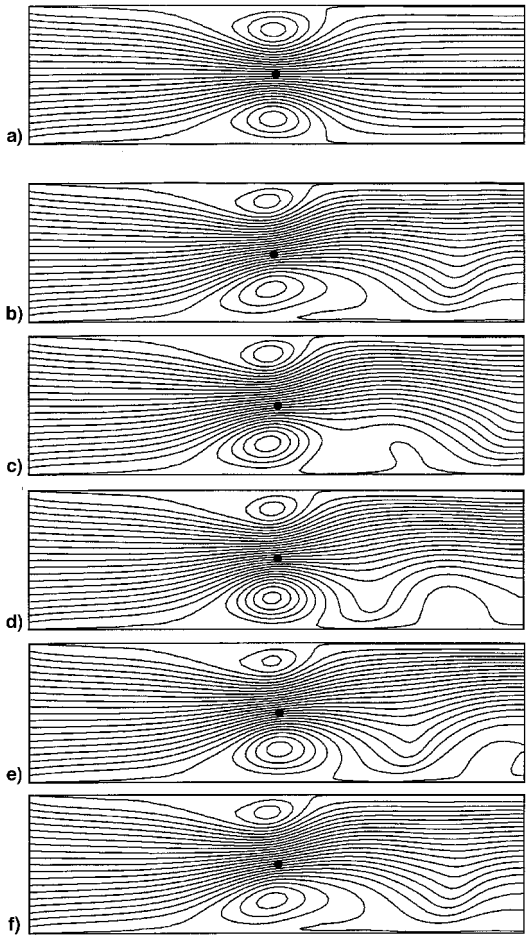


**Fig. 3 Variation of flowfield with time ($V_0 = 17.5$ kV, $Re = 1.8 \times 10^3$): a) $Gr = 0$; b) $Gr = 10^4$, $\tau = 609.38$; c) $\tau = 618.75$; d) $\tau = 628.12$; e) $\tau = 637.5$; and f) $\tau = 646.88$.**

EHD number increases. This transition in the flowfield is consistent with what has been observed in the forced convection.[7] For a given EHD number, an increase in the thermal buoyancy strength also leads to a more unstable flowfield.

The effect of thermal buoyancy on the flow stability can be examined directly from the variation of flow and temperature fields with time. At $V_0 = 15$ kV and $Re = 1.8 \times 10^3$ ($N_{ehd} = 1.69$), a steady state is reached when thermal buoyancy is absent. Although a steady state is maintained when the thermal buoyancy strength increases, it is noticed that thermal buoyancy does not have a significant effect on the flow and temperature fields (and thus the heat transfer results) until the Grashof number is increased to $10^6$. At $V_0 = 17.5$ kV and $Re = 1.8 \times 10^3$ ($N_{ehd} = 2.62$), the flow and temperature fields also reach a steady state in the absence of thermal buoyancy. However, they become oscillatory when the Grashof number is increased to $10^6$ (Figs. 3 and 4). It is clear from the figures that the oscillation in the flow and temperature fields is a result of the repeated occurrence of thermal disturbance in the lower boundary. The period of oscillation in this case is about 37.5 dimensionless time as determined from the time-evolution plot of the Nusselt number.

For $V_0 = 12.5$ kV and $Re = 6 \times 10^2$ ($N_{ehd} = 8.33$), the flow and temperature fields exhibit an oscillatory nature even when thermal buoyancy is absent. As reported earlier,[5] this flow instability is induced solely by the electric body force. Although oscillatory, the flow and temperature fields are symmetric to the centerline because of the absence of thermal buoyancy. With the inclusion of thermal buoyancy, the flow and temperature fields remain oscillatory, but the symmetric structure is no longer preserved (Figs. 5 and 6). It is interesting to note

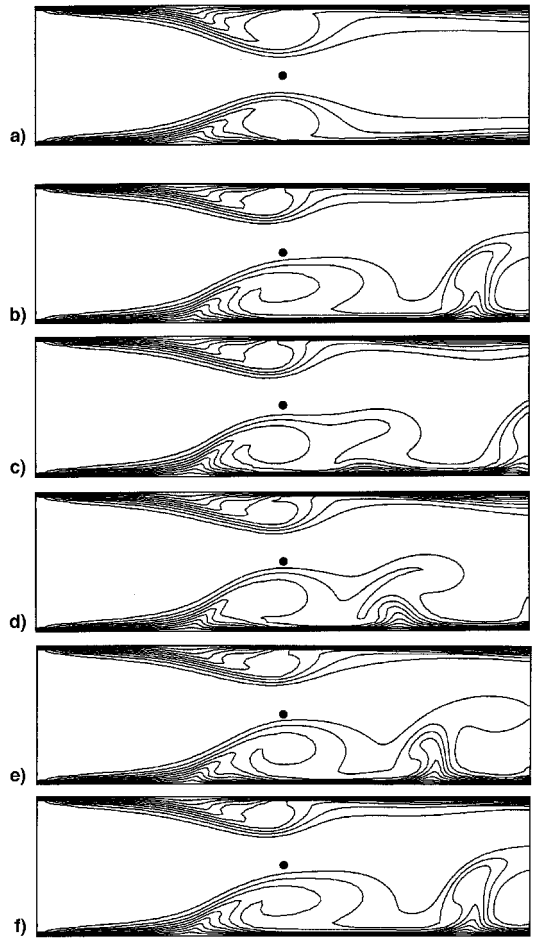


**Fig. 4 Variation of temperature field with time ($V_0 = 17.5$ kV, $Re = 1.8 \times 10^3$): a) $Gr = 0$; b) $Gr = 10^4$, $\tau = 609.38$; c) $\tau = 618.75$; d) $\tau = 628.12$; e) $\tau = 637.5$; and f) $\tau = 646.88$.**

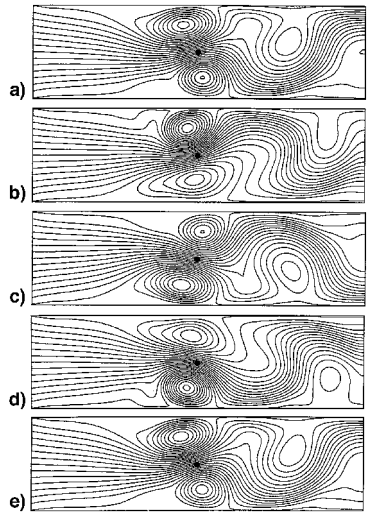


**Fig. 5 Variation of flowfield with time ($V_0 = 12.5$ kV, $Re = 6 \times 10^2$, $Gr = 10^4$). $\tau$ = a) 909.38, b) 918.75, c) 928.12, d) 937.50, and e) 946.88.**

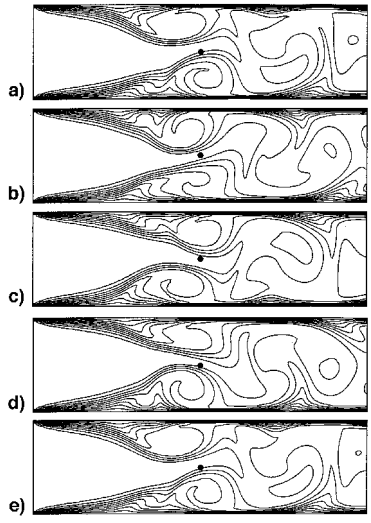


**Fig. 6 Variation of temperature field with time ($V_0 = 12.5$ kV, $Re = 6 \times 10^2$, $Gr = 10^4$). $\tau$ = a) 909.38, b) 918.75, c) 928.12, d) 937.50, and e) 946.88.**

that, at a low Reynolds number, a small increase in the thermal buoyancy strength, e.g., $Gr = 10^4$ in the present case, can cause a dramatic change in the flow and temperature fields. The added thermal buoyancy has not only changed the period of oscillation from 32.5 to 37.5 dimensionless time, but has also increased the extent of flow mixing. Notice that the flow mixing in this case extends over nearly the entire channel as compared with that only limited to the lower boundary in the previous case. As a result, it leads to a considerable increase in heat transfer.

To examine the effect of thermal buoyancy on the heat transfer enhancement, the variations of overall Nusselt number with time are presented. For example, at $V_0 = 15$ kV and $Re = 1.8 \times 10^3$ ($N_{ehd} = 1.69$), the flow and temperature fields reach a steady state in the absence of thermal buoyancy. With an increase in the thermal buoyancy strength, it is noticed that the overall Nusselt number remains almost the same until the Grashof number is raised to $10^6$. For $V_0 = 15$ kV and $Re = 1.2 \times 10^3$ ($N_{ehd} = 3.80$), the flow and temperature fields in the absence of thermal buoyancy oscillate with a period of $\tau_p \simeq 32.5$ (Fig. 7). It is observed that the oscillation in the flow and temperature fields becomes intensified with an increase in the thermal buoyancy strength. Not only the period but also the

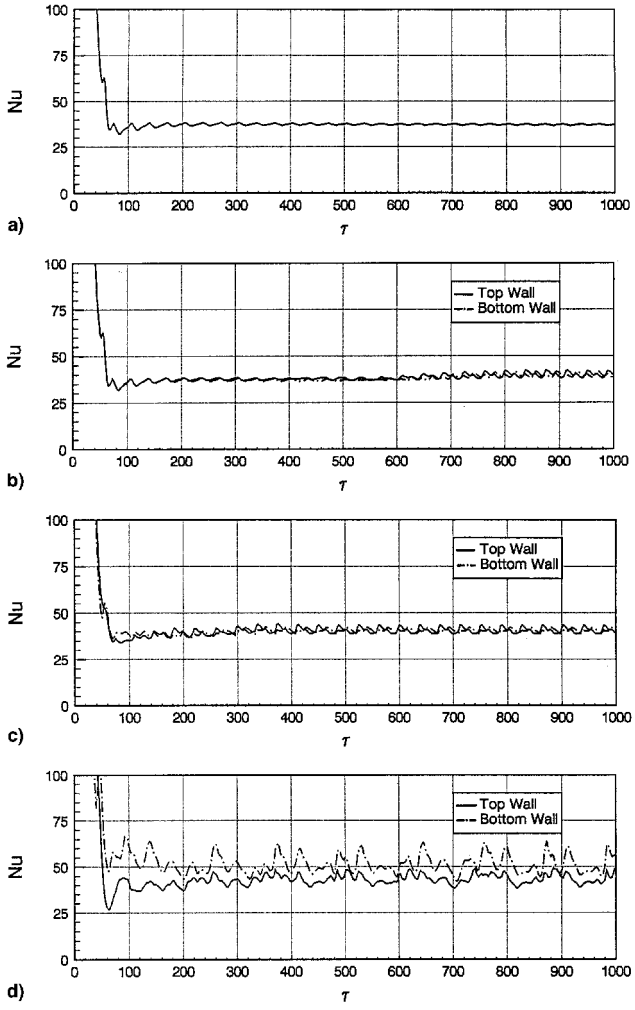


**Fig. 7 Variation of average Nusselt number with time ($V_o$ = 15 kV, $Re$ = 1.2 × $10^3$). $Gr$ = a) 0, b) $10^4$, c) $10^5$, and d) $10^6$.**

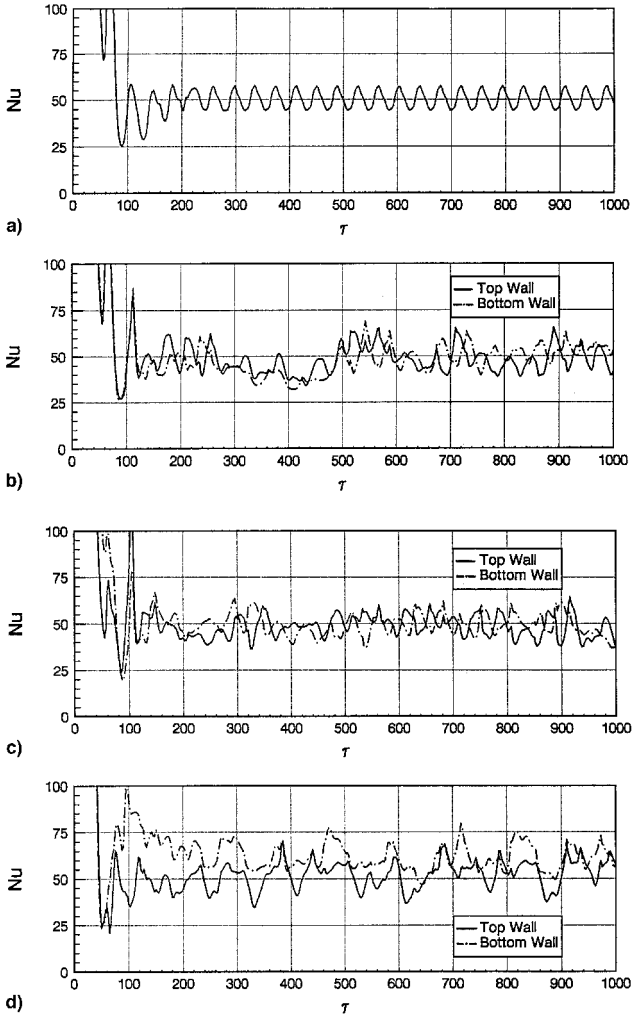


**Fig. 8 Variation of average Nusselt number with time ($V_o$ = 15 kV, $Re$ = 6 × $10^2$). $Gr$ = a) 0, b) $10^4$, c) $10^5$, and d) $10^6$.**

amplitude of the oscillation increases. The flow and temperature fields finally develop into a nonperiodic oscillation at $Gr$ = $10^6$. A similar transition in the flow and temperature fields can be observed from Fig. 8 for $Re$ = 6 × $10^2$ ($N_{ehd}$ = 15.21). Because of the weak flow inertia, the transition to nonperiodic state occurs at a small Grashof number $Gr$ = $10^4$.

To evaluate the effect of thermal buoyancy on the EHD-enhanced heat transfer, the overall Nusselt number obtained are compared with those of forced convection at the same conditions. It has been reported that EHD heat transfer enhancement in forced convection (for the same geometry) ranges from 8 to 270%, depending on the flow and electric field conditions.[7] It is important to note that the overall Nusselt number obtained in the present study for pure forced convection in general agree well with those reported by Shah and London.[11] For example, the predicted Nusselt number is within 6% of that reported in the literature for $Re$ = 1.8 × $10^3$. The differences observed may be attributed to the neglect of axial diffusion in the previous study.[11]

For periodic flows, the time-averaged overall Nusselt number has been calculated using the following expression:

$$\overline{Nu} = \frac{1}{\tau_p}\int_{\tau}^{\tau+\tau_p} Nu \, dt \tag{13}$$

while for nonperiodic flows, it is calculated by

$$\overline{Nu} = \frac{1}{\tau_T}\int_{0}^{\tau_T} Nu \, dt \tag{14}$$

where $\tau_p$ is the period of the oscillation, and $\tau_T$ is the entire time span. It is observed that, as $\tau_T$ becomes sufficiently large, the average Nusselt number based on Eq. (14) approaches an asymptotic value.

The time-averaged overall Nusselt number ratios are shown in Fig. 9 as a function of the mixed convection parameter $Gr/Re^2$. The overall Nusselt numbers shown are the sum of the overall Nusselt number on the top and bottom walls. In these figures the solid symbols denote steady flows, open symbols denote periodic flows, and half-filled symbols represent nonperiodic flows. When compared with the EHD-enhanced forced convection, it can be seen that thermal buoyancy has a negligible effect on the heat transfer enhancement at the forced convection dominant regime, i.e., $Gr/Re^2 \ll 1$. Its effect becomes noticeable at a higher applied voltage or when $Gr/Re^2 \geq 1$. It is also noticed that the heat transfer enhancement by oscillatory flows is usually higher than that by steady flows. As discussed earlier, flows tend to be oscillatory at a large EHD number. An added thermal buoyancy in these cases can lead to a further increase in the heat transfer enhancement by providing additional fluid mixing.

When compared with pure forced convection, it is found that the heat transfer enhancement increases with the voltage applied, but decreases if the flow Reynolds number is increased. At a high voltage, the flow and temperature fields tend to become oscillatory, particularly at the presence of thermal buoyancy. The combined effects of electric field and thermal buoyancy can increase heat transfer more than three times of that of pure forced convection.

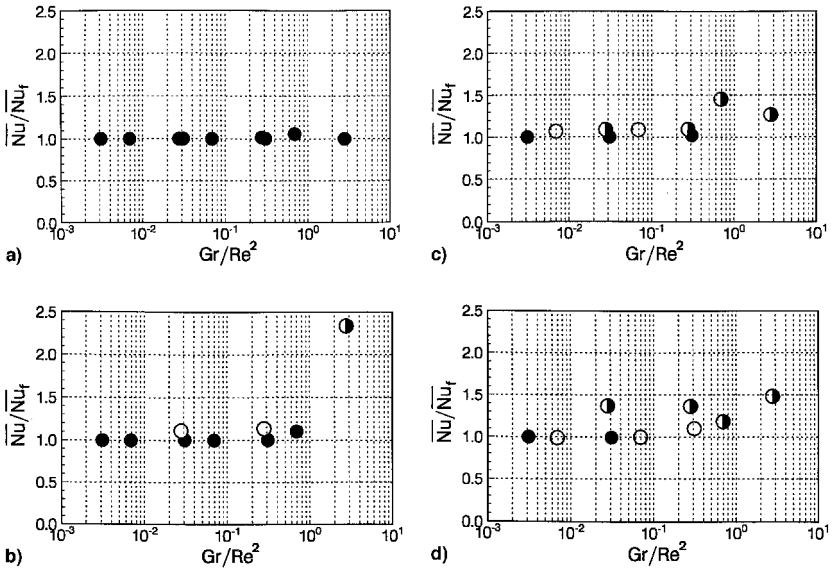


**Fig. 9 Effects of thermal buoyancy on the EHD-enhanced forced convection. $V_0$ = a) 10, b) 12.5, c) 15, and d) 17.5 kV.**

## Conclusions

Numerical results have been presented for mixed convection in a horizontal channel under the influence of an electric field. Depending on the flow Reynolds number, Grashof number, and EHD number, the flow and temperature fields may become steady, periodic, or nonperiodic. When the flow inertia is weak, i.e., at a high EHD number, the flow and temperature fields exhibit an oscillatory nature. With the addition of thermal buoyancy, the flow and temperature fields become more unstable. It has been shown that an enhancement in heat transfer is possible because of the oscillation of the flowfield. The maximum enhancement in heat transfer that resulted from the combined effects of the electric field and thermal buoyancy is more than three times that of pure forced convection.

While the present study has explored a fundamental problem in EHD-enhanced heat transfer as an extension of several earlier studies, the results have some interesting implications for important problems of electrostatic precipitation. Generally, the particle-laden exhaust gas from numerous industrial applications is at an elevated temperature. During the gas cleaning process using an electrostatic precipitator, thermal buoyancy resulting from such a large temperature gradient may lead to a serious flow instability that could significantly reduce the particle collection efficiency. To overcome this problem, it is suggested that a wet-type precipitator be used or the exhaust gas be cooled before it is passed through the precipitator.

## Acknowledgment

The author gratefully acknowledges the financial support received from the University of Oklahoma Research Council through the Junior Faculty Summer Research Fellowship. The support of supercomputing provided by Cray Research Inc., administrated through Michael D. Tuttle, is gratefully acknowledged. The assistance in computation by M. Johnson and J. M. Zhang is also gratefully acknowledged.

## References

[1]Jones, T. B., "Electrohydrodynamically Enhanced Heat Transfer in Liquids—A Review," *Advances in Heat Transfer*, Vol. 14, 1978, pp. 107–148.

[2]Davidson, J. H., Kulacki, F. A., and Dunn, P. F., "Convective Heat Transfer with Electric and Magnetic Fields," *Handbook of Single-Phase Convective Heat Transfer*, edited by S. Kakac et al., Wiley, New York, 1987, pp. 1–47.

[3]Yabe, A., Mori, Y., and Hijikata, K., "Active Heat Transfer Enhancement by Utilizing Electric Fields," *Annual Review of Heat Transfer*, Vol. 7, 1996, pp. 193–244.

[4]Yamamoto, T., and Velkoff, H. R., "Electrohydrodynamics in an Electrostatic Precipitators," *Journal of Fluid Mechanics*, Vol. 108, July 1981, pp. 1–8.

[5]Lai, F. C., McKinney, P. J., and Davidson, J. H., "Oscillatory Electrohydrodynamic Gas Flows," *Journal of Fluids Engineering*, Vol. 117, Sept. 1995, pp. 491–497.

[6]Takimoto, A., Tada, Y., and Hayashi, Y., "Convective Heat Transfer Enhancement by a Corona Discharge," *Heat Transfer—Japanese Research*, Vol. 20, No. 1, 1991, pp. 18–35.

[7]Lai, F. C., "Heat Transfer Enhancement by EHD-Induced Oscillatory Flows," *International Journal of Heat and Mass Transfer* (submitted for publication).

[8]Kulkarni, S. S., and Lai, F. C., "Effects of Electric Field on Mixed Convection in a Vertical Channel," *Proceedings of the 1995 National Heat Transfer Conference*, Vol. 8, HTD-Vol. 310, American Society of Mechanical Engineers, New York, 1995, pp. 59–67, Chap. 9.

[9]Jaluria, Y., and Torrance, K. E., *Computational Heat Transfer*, Hemisphere, New York, 1986.

[10]Davidson, J. H., and Shaughnessy, E. J., "Turbulence Generation by Electric Body Forces," *Experiments in Fluids*, Vol. 4, No. 1, 1986, pp. 17–26.

[11]Shah, R. K., and London, A. L., "Laminar Flow Forced Convection in Ducts," *Advances in Heat Transfer*, Supplement 1, Academic, New York, 1978.